Kinetics and mechanism of the hydrogen peroxide oxidation of a pentafluorophenyl-substituted iron(III) porphyrin †

Ian D. Cunningham,*[a] Timothy N. Danks,[a] Keith T. A. O'Connell[a] and Peter W. Scott[b]

[a] *Department of Chemistry, School of Physical Sciences, University of Surrey, Guildford, Surrey, UK GU2 5XH. E-mail: i.cunningham@surrey.ac.uk*
[b] *Chemical Development Division, GlaxoWellcome Medicines Research Centre, Stevenage, Herts, UK SG1 2NY*

Received (in Cambridge) 4th May 1999, Accepted 15th July 1999

Kinetic analysis of the (F_{20}TPP)FeCl-catalysed H_2O_2 oxidation of 3-hydroxy-2-(*trans*-4-*tert*-butylcyclohexyl)-methylnaphtho-1,4-quinone is consistent with rapid reaction of the organic substrate with an oxoperferryl intermediate [(F_{20}TPP$^{\bullet+}$)Fe^{IV}=O] formed in the first and rate-limiting step. A second-order rate constant for oxidation of the catalyst of 22 ± 5 dm^3 mol^{-1} s^{-1} is found, a value lower than previously reported. In the absence of the organic substrate, H_2O_2 oxidises the catalyst to an oxoferryl species (F_{20}TPP)Fe^{IV}=O, probably *via* the oxoperferryl species. This oxoferryl compound is itself bleached by H_2O_2 with a second-order rate constant of 0.081 ± 0.004 dm^3 mol^{-1} s^{-1} probably involving oxidation of the porphyrin ring.

Introduction

The metalloporphyrin (F_{20}TPP)FeCl (**1**)‡ is a readily-

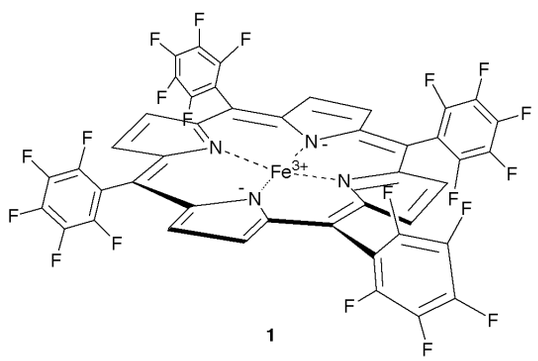

1

available and efficient catalyst for the oxidation of organic substrates;[1] it is soluble in organic solvents and apparently robust. This catalyst is, therefore, one of the most popular *cytochrome P-450* mimics for oxidation (electron removal),[2] oxygenation,[2,3] hydroxylation,[4] cyclopropanylation[5] and radical formation.[6] A variety of oxidants are compatible, including iodosylbenzenes,[1a,2,3a,b,6,7] dioxygen,[1a,4,8] hydrogen peroxide,[1a,2,3a,b] hydroperoxides[1a,2,3a] and peracids.[1a,2,3a,9] Most mechanistic studies have concentrated on the use of the iodosylbenzene,[2,3a,7,10] hydroperoxide[2,3a,10] and peracid oxidants.[2,3a,10] Despite qualitative indications of some stability for **1** in the presence of the clean but vigorous oxidant hydrogen peroxide,[2,3a,11] only limited kinetic and mechanistic studies of its catalytic ability and stability have been reported.[2,3a]

In this paper we present a study of the kinetics and mechanism of the (F_{20}TPP)FeCl–H_2O_2 reaction, both in the absence and in the presence of a hydroxynaphthoquinone substrate **2**. This substrate was found in our earlier work to be readily epoxidised by this catalyst and oxidant (Scheme 1).[12]

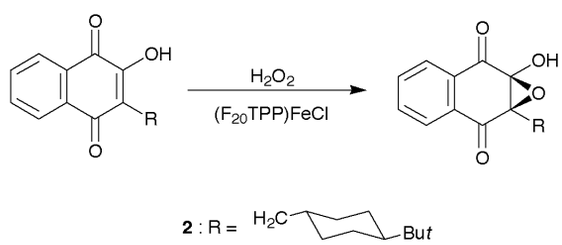

Scheme 1

Experimental

Materials

Methanol (HPLC grade) and dichloromethane (general purpose grade) solvents were obtained from Fisons and were used as received. Catalyst F_{20}TPPFeCl was from Aldrich and was used as received. Hydrogen peroxide (30% w/v) was purchased from BDH Laboratory Supplies; concentrations of solutions prepared from stock were determined by UV-Vis spectroscopy (ε_{242} = 39.4 dm^3 mol^{-1} cm^{-1}). Stock solutions of catalyst F_{20}TPPFeCl in methanol were prepared. Samples of 3-hydroxy-2-(*trans*-4-*tert*-butylcyclohexyl)methylnaphtho-1,4-quinone **2** and 3-hydroxy-2-cycloheptylnaphtho-1,4-quinone were gifts from GlaxoWellcome and were used as received after checking for purity by ^{1}H NMR and TLC.

Apparatus

All UV-Vis spectra and kinetic experiments were recorded using a thermostatted Philips PU87 spectrometer; kinetic data were downloaded to a PC for processing using Microsoft Excel. Quartz UV cuvettes (max. volume *ca.* 3 cm^3) were of path length 10.0 mm and were capped with Teflon stoppers. Aliquots of stock solutions were injected using 25 and 100 mm^3 microsyringes.

Preliminary repscans

In general, all kinetic experiments were preceded by repscans to establish appropriate wavelengths for monitoring. A typical experiment (oxidation of F_{20}TPPFeCl with H_2O_2 in methanol

† Details of the kinetic analyses are available from the RSC web site, see http://www.rsc.org/suppdata/p2/1999/2133/
‡ (F_{20}TPP)FeCl = [5,10,15,20-Tetrakis(pentafluorophenyl)-21*H*,23*H*-porphine]iron(III) chloride.

without hydroxynaphthoquinone **2**) was carried out as follows. A quartz cuvette was charged with methanol (2.0 cm^3) using a volumetric pipette. Subsequently, catalyst (25 mm^3 of 3.4×10^{-4} mol dm^{-3} stock in chloroform, to give 4.2×10^{-6} mol dm^{-3} in cell) was injected using a 25 mm^3 syringe. After allowing *ca.* 5 min. for temperature equilibration (25 °C), the absorbance spectrum 350–470 nm was recorded. Aqueous hydrogen peroxide (2.5 mm^3 of 0.175 mol dm^{-3} stock, to give 2.2×10^{-4} mol dm^{-3} in cell) was injected (25 mm^3 syringe) and the UV-Vis spectrum recorded after 15 s, then every 1 min for 20 min.

Oxidation of 3-hydroxy-2-(*trans*-4-*tert*-butylcyclohexyl)methylnaphtho-1,4-quinone

Kinetic experiments. To quartz cuvettes, charged by volumetric pipette with 3:1 (v/v) methanol–dichloromethane (2.0 cm^3), were injected by microsyringe volumes (6–18 mm^3) of stock **2** [1.59×10^{-2} mol dm^{-3} in 3:1 (v/v) methanol–dichloromethane] and (0–13 mm^3) of stock catalyst **1** [1.07×10^{-3} mol dm^{-3} in 3:1 (v/v) methanol–dichloromethane] to give the concentrations shown in Table 1. After allowing *ca.* 5 min for thermal equilibration at 25 °C, reactions were initiated by injection of volumes (0–8 mm^3) of stock aqueous hydrogen peroxide (1.56×10^{-1} mol dm^{-3}) to give the concentrations in Table 1. The absorbance (A) readings at 283 nm were monitored until steady A_∞ readings were reached (up to 2.5 h). *A vs. t* plots, typified by Fig. 1, were analysed as detailed in the Results section.

Oxidation of catalyst by hydrogen peroxide

Kinetic experiments: initial rates method (variation of hydrogen peroxide concentration). A stoppered quartz cuvette was charged with methanol (2.0 cm^3) and catalyst (25 mm^3 of 3.4×10^{-4} mol dm^{-3} stock in chloroform, to give 4.1×10^{-6} mol dm^{-3} in cell) and allowed to come to equilibrium at 25 °C before addition of aqueous hydrogen peroxide (24, 50 or 100 mm^3 of 2.0×10^{-1} mol dm^{-3} stock, *or* 75 or 100 mm^3 of 3.9×10^{-1} mol dm^{-3} stock) to give a series of reaction solutions with the $[H_2O_2]_0$ in cell: 2.3×10^{-3}, 4.7×10^{-3}, 9.3×10^{-3}, 1.41×10^{-2} and 1.85×10^{-2} mol dm^{-3}. The absorbance at 408 nm was measured after 15 s, then typically, every 10 s for 5 min. Similar experiments were carried out under the same conditions at $[H_2O_2]_0$: 2.1×10^{-3}, 4.2×10^{-3}, 8.2×10^{-3}, 1.3×10^{-2} and 1.7×10^{-2} mol dm^{-3}. The resulting plots of *A vs. t*, typified by the *inset* to Fig. 4, were analysed as in the Results section. Data from the early part of the reactions yielded the rate constants in Table 4, while those from the later part yielded some of the dA/dt values in Table 2.

Kinetic experiments: first-order method (variation of hydrogen peroxide concentration). For certain runs (those at $[H_2O_2]_0 = 2.3 \times 10^{-3}$, 4.7×10^{-3}, 9.3×10^{-3}, 1.41×10^{-2} and 1.85×10^{-2} mol dm^{-3}) monitoring was continued until bleaching of the Soret peak was complete (see Fig. 4). The *A vs. t* data were treated by a first-order analysis, as described in the Results section, to give the rate constants in Table 3.

Kinetic experiments: initial rates method (variation of catalyst concentration). Similar experiments at $[H_2O_2]_0 = 4.2 \times 10^{-3}$ mol dm^{-3} and $[\text{catalyst}]_0 = 1.7 \times 10^{-6}$, 2.5×10^{-6}, 3.3×10^{-6} and 4.1×10^{-6} mol dm^{-3} gave some of the dA/dt_0 values in Table 2.

Error analysis

All runs were carried out in at least duplicate and the values of dA/dt or rate constant given in the tables are the average of the runs with the standard deviation quoted as the uncertainty. Uncertainties quoted in the text for derived quantities (*e.g.* second-order rate constants) are either standard deviations from duplicate runs or the normal mathematical combination of the standard deviations of the parameters used to calculate the relevant quantity, whichever is the greater (unless otherwise discussed in the text).

Table 1 Values of dA/dt_0 at $\lambda = 283$ nm for the (F_{20}TPP)FeCl-catalysed H_2O_2 oxidation of 3-hydroxy-2-(*trans*-4-*tert*-butylcyclohexyl)methylnaphtho-1,4-quinone (**2**) in 3:1 (v/v) methanol–dichloromethane at 25 °C

Entry	$[H_2O_2]_0/10^{-6}$ mol dm^{-3}	$[\mathbf{1}]_0/10^{-6}$ mol dm^{-3}	$[\mathbf{2}]_0/10^{-6}$ mol dm^{-3}	$(dA/dt_0)/10^{-4}$ s^{-1}
1	0	5.4	130	0[a]
2	154	5.4	130	−2.6 ± 0.1
3	307	5.4	130	−5 ± 1.5
4	461	5.4	130	−7.9 ± 3.0
5	613	5.4	130	−8 ± 1
6	615	0	130	0[a]
7	615	2.7	130	−2.7 ± 0.5
8	615	4.1	130	−5.4 ± 1.6
9	615	5.4	130	−7.4 ± 0.9
10	615	6.8	130	−11.6 ± 5.4
11	617	5.4	47	−6.8 ± 2.7
12	617	5.4	79	−8.6 ± 0.3
13	617	5.4	110	−9.8 ± 2.4
14	617	5.4	141	−9.6 ± 0.9

[a] No reaction in the absence of either H_2O_2 or **1**.

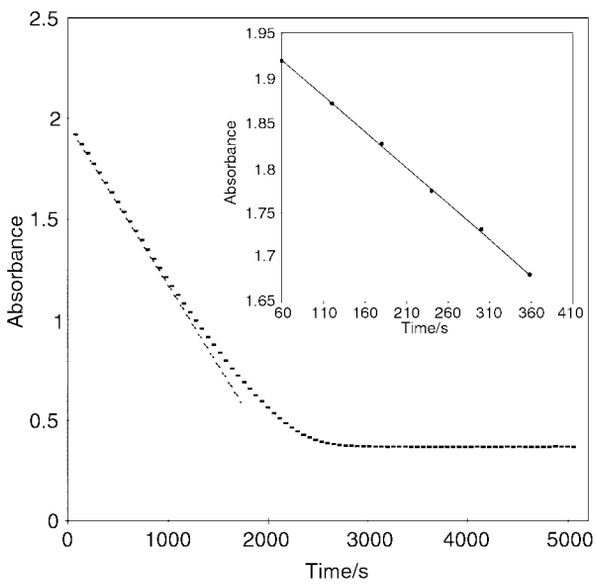

Fig. 1 Plot of absorbance change at 283 nm *vs.* time for the (F_{20}TPP)FeCl-catalysed H_2O_2 oxidation of **2** in 3:1 methanol–dichloromethane at 25 °C. $[\mathbf{2}]_0 = 130 \times 10^{-6}$ mol dm^{-3}, $[\mathbf{1}]_0 = 5.4 \times 10^{-6}$ mol dm^{-3}, $[H_2O_2]_0 = 615 \times 10^{-6}$ mol dm^{-3}. Inset. Expansion to show the first 15% of the reaction.

Results

Oxidation of alkylhydroxynaphthoquinone

First, we studied the catalyst oxidation indirectly by monitoring the (F_{20}TPP)FeCl-catalysed H_2O_2 oxidation of 3-hydroxy-2-(*trans*-4-*tert*-butylcyclohexyl)methylnaphtho-1,4-quinone (**2**). Evidence has already been presented to show that this substrate is *efficiently* oxidised (epoxidised) by this catalyst and oxidant and a UV-Vis repscan showed loss of the hydroxynaphthoquinone peak at 283 nm (due presumably to the loss of the chromophore on epoxidation) in excess H_2O_2 in methanol–dichloromethane (3:1 v/v).[12] A plot of absorbance *vs.* time at 283 nm is shown in Fig. 1 and similar plots were obtained for the same reaction at the various concentrations of catalyst **1**, H_2O_2 and **2** as shown in Table 1.

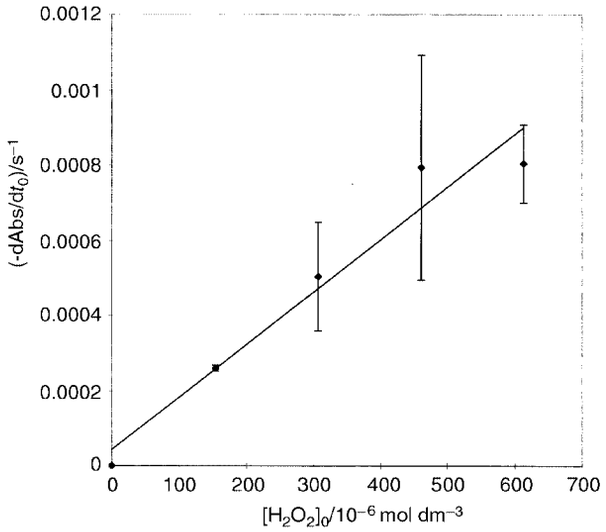

Fig. 2 Plot of $-dA/dt_0$ *vs.* $[H_2O_2]_0$ for the $(F_{20}TPP)FeCl$-catalysed H_2O_2-oxidation of **2** in 3:1 (v/v) methanol–dichloromethane at 25 °C. $[\mathbf{2}]_0 = 130 \times 10^{-6}$ mol dm^{-3}, $[\mathbf{1}]_0 = 5.4 \times 10^{-6}$ mol dm^{-3}, $[H_2O_2]_0 = 0$ to 613×10^{-6} mol dm^{-3}.

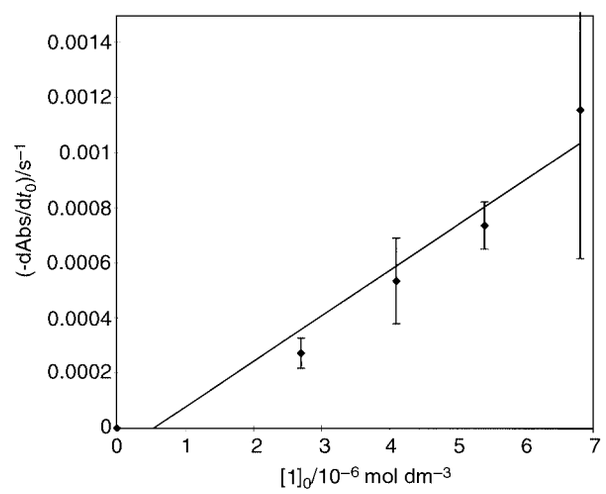

Fig. 3 Plot of $-dA/dt_0$ *vs.* $[\mathbf{1}]_0$ for the $(F_{20}TPP)FeCl$-catalysed H_2O_2 oxidation of **2** in 3:1 (v/v) methanol–dichloromethane at 25 °C. $[\mathbf{2}]_0 = 130 \times 10^{-6}$ mol dm^{-3}, $[H_2O_2]_0 = 615 \times 10^{-6}$ mol dm^{-3}, $[\mathbf{1}]_0 = 0$ to 6.8×10^{-6} mol dm^{-3}.

A cursory glance at Fig. 1 shows that the decrease in absorbance does not fit cleanly a simple first- or second-order kinetic pattern. Indeed rather complex absorbance *vs*. time plots seem to be a feature of such reactions.[3a] Complicating factors might include catalyst decomposition and additional H_2O_2 decomposition (*e.g.* catalase-type dismutation which would reduce the concentration of H_2O_2 *without* resulting loss of hydroxynaphthoquinone absorbance at 283 nm). To minimise such problems the method of 'initial-rate' was used[13] and analysis of the data by this method gives linear plots typified by that shown as the inset to Fig. 1.§ The data, values of dA/dt_0, at varying initial concentrations of the reactions components, H_2O_2, $(F_{20}TPP)FeCl$ (**1**) and substrate (**2**) are collected in Table 1 and plotted in Figs. 2 (dA/dt *vs*. $[H_2O_2]_0$; entries 1–5) and 3 (dA/dt *vs*. $[\mathbf{1}]_0$; entries 6–10). Despite the rather large scatter in the points of Figs. 2 and 3, it is clear that the data are best fitted by a first-order dependence of dA/dt_0 on the concentration of H_2O_2 and of catalyst **1**.

§ Data was taken within the first 5–15% of the reaction. Strictly speaking, the initial-rate method should use only up to *ca.* 5%, but as will be seen, the plots were linear up to >50% of reaction.

In contrast the dependence on [**2**] (entries 11–14 in Table 1) was, at higher levels of **2**, approximately zero-order and overall we propose that dA/dt is given by eqn. (1). Since it is reasonable

$$dA/dt \propto [H_2O_2][(F_{20}TPP)FeCl] \quad (1)$$

to expect that, *during the early part of the reaction*, (i) $[(F_{20}TPP)FeCl]$ is constant (although *vide infra*) and (ii) H_2O_2 is in excess, eqn. (1) should result in an apparent zero-order plot of *A vs.* time. This is clearly reflected in the plot of Fig. 1 in which the broken line illustrates the continuation of the 'initial' linearity of the *A vs.* time plot to over 50% of the reaction.

The form of eqn. (1) is consistent with the generally-accepted mechanism of metalloporphyrin-catalysed oxidation shown in Scheme 2 which involves slow rate-limiting conversion of

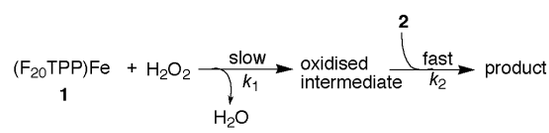

Scheme 2

the catalyst to an oxidised intermediate which then transfers oxygen to the naphthoquinone substrate in a fast step.

For Scheme 2 it can be shown that dA/dt is given by eqn. (2)

$$-dA/dt = \{(A_0 - A_\infty)/[2]_0\}k_1[H_2O_2][(F_{20}TPP)FeCl] \quad (2)$$

where k_1 is the second-order rate constant for oxidation of catalyst **1**.¶

The value of the term $(A_0 - A_\infty)/[\mathbf{2}]_0$ was found to be 12200 ± 460 dm^3 mol^{-1}. From the slope of the dA/dt_0 *vs.* $[H_2O_2]_0$ at constant $[\mathbf{1}]_0$ plot (Fig. 2) a value for k_1 of 21 dm^3 mol^{-1} s^{-1} can be calculated; while the dA/dt_0 *vs.* $[\mathbf{1}]_0$ plot (Fig. 3) gives k_1 as 21 dm^3 mol^{-1} s^{-1}. Despite the apparent close agreement, the uncertainty in the raw data averages *ca.* ± 20% as do the accumulated uncertainties in derived values (resulting from the standard deviations to the slopes of Figs. 2 and 3, concentrations *etc.*). In view of this we quote a value for k_1 of 22 ± 5 dm^3 mol^{-1} s^{-1}. It should be noted that this value is significantly lower than that obtained by Traylor under similar conditions of solvent and oxidant, but using 2,4,6-tri(*tert*-butyl)phenol or β-carotene as substrate.[2]

The findings were checked by repeating the experiments using the related 2-cycloheptyl-3-hydroxynaphtho-1,4-quinone as substrate. The results at $[\mathbf{1}] = 5.5 \times 10^{-6}$ mol dm^{-3}, $[H_2O_2] = 620 \times 10^{-6}$ mol dm^{-3} and [2-cycloheptyl-3-hydroxynaphtho-1,4-quinone] $= 120 \times 10^{-6}$ mol dm^{-3} were treated according to eqn. (1) to yield a value for k_1 of 25 dm^3 mol^{-1} s^{-1}. However, absorbance changes for this substrate, although of the same order of magnitude as for **2**, were less precise and appeared to show an initial slower rate of change of absorbance giving sigmoidal curves in many cases.‖

Catalyst oxidation in the absence of substrate

We then turned our attention to oxidation of the catalyst **1** in the *absence* of organic reductant (such as **2**). Treatment of micromolar $(F_{20}TPP)FeCl$ in methanol with millimolar H_2O_2 resulted in bleaching over several hours as shown by disappearence of the Soret band of the metalloporphyrin at 404 nm. On closer inspection, the bleaching was seen to be preceded by a rapid shift of the 404 nm peak to one at *ca*. 408 nm over *ca.*

¶ Derivations of kinetic equations are shown in the supplementary material. See note †.

‖ See Figure Supp1 in the supplementary material. See note †.

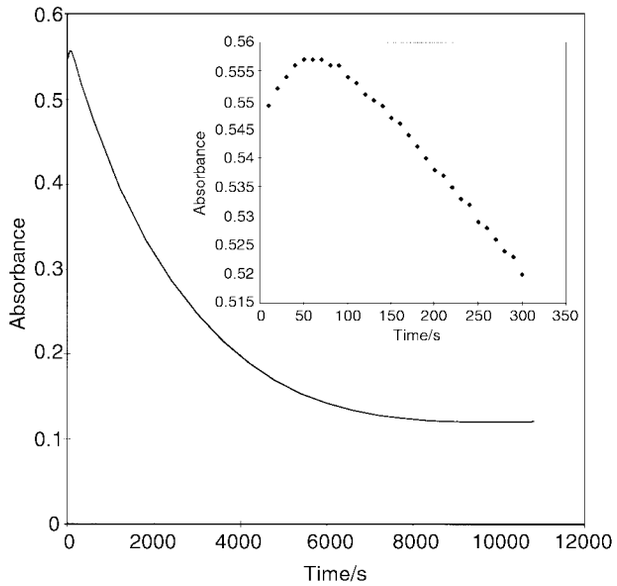

Fig. 4 Plot of absorbance change at 408 nm *vs.* time for the H_2O_2 oxidation of (F_{20}TPP)FeCl (**1**) in methanol at 25 °C. $[H_2O_2]_0 = 4.7 \times 10^{-3}$ mol dm^{-3}, $[\mathbf{1}]_0 = 4.1 \times 10^{-6}$ mol dm^{-3}. Inset. Expansion to show the first 300 s of the reaction.

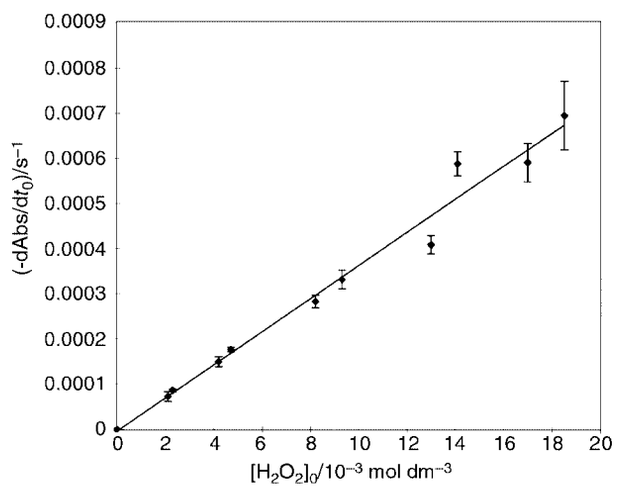

Fig. 5 Plot of $-dA/dt_0$ *vs.* $[H_2O_2]_0$ for the H_2O_2 oxidation of rapidly-formed 408 nm peak in methanol at 25 °C. $[\mathbf{1}]_0 = 4.1 \times 10^{-6}$ mol dm^{-3}, $[H_2O_2]_0 = 2.1$ to 18.5×10^{-3} mol dm^{-3}.

1 min.** This is illustrated by Fig. 4 and its inset, in which the absorbance change at 408 nm for the initial 5% of the reaction is shown.

Attention was firstly focussed on the slower second reaction. Once again for the reasons outlined above *and* to determine the reaction order, the kinetics were analysed using the initial-rate method *omitting the few minutes involving the rapid 404 to 408 nm shift* (see Fig. 4). Values of the initial rate dA/dt_0 for this second reaction are given in Table 2.

Values of dA/dt_0 at fixed $[\mathbf{1}]_0$ are plotted in Fig. 5 *vs.* $[H_2O_2]_0$ and in Fig. 6 *vs.* $[\mathbf{1}]_0$ at fixed $[H_2O_2]_0$. It is clear from the plots that dA/dt_0 for this reaction (loss of the compound absorbing at 408 nm) is linear in $[H_2O_2]_0$ and in $[\mathbf{1}]_0$. It is also reasonable to assume that the compound absorbing at 408 nm is rapidly formed from **1** and stoichiometrically equivalent to **1**, so that the observed form of the rate equation is given by eqn. (3),

$$dA/dt \propto [H_2O_2][(F_{20}TPP)Fe_{408}] \quad (3)$$

** Overall, a repscan during the first minute or so showed the spectrum of **1** (λ_{max} = 404, 485 and 580 nm) to be transformed into that of an intermediate (λ_{max} = 408 and 550 nm) before slower bleaching.

Table 2 Values of dA/dt_0 at $\lambda = 408$ nm for the H_2O_2 oxidation of (F_{20}TPP)FeCl (**1**) in methanol at 25 °C[a]

Entry	$[H_2O_2]_0/10^{-3}$ mol dm^{-3}	$[\mathbf{1}]_0$[b]$/10^{-6}$ mol dm^{-3}	$(dA/dt_0)/10^{-5}$ s^{-1}
1	2.1	4.1	7 ± 1
2	2.3	4.1	8.6 ± 0.3
3	4.2	4.1	15 ± 1
4	4.7	4.1	17.6 ± 0.5
5	8.2	4.1	28 ± 1
6	9.3	4.1	33 ± 2
7	13.0	4.1	41 ± 2
8	14.1	4.1	59 ± 3
9	17.0	4.1	59 ± 4
10	18.5	4.1	70 ± 8
11	4.2	1.7	6.14 ± 0
12	4.2	2.5	9.15 ± 0.04
13	4.2	3.3	11.4 ± 0.6
14	4.2	4.1	14.6 ± 0.9

[a] Omitting the small initial *increase* in absorbance due to formation of the 408 nm peak. [b] Concentration of (F_{20}TPP)FeCl added initially.

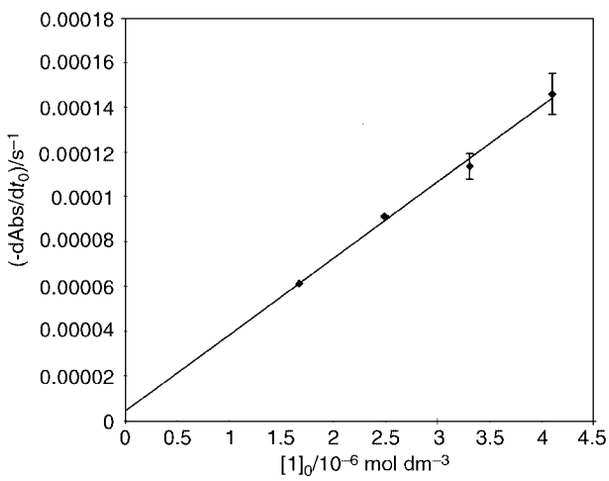

Fig. 6 Plot of $-dA/dt_0$ *vs.* $[\mathbf{1}]_0$ for the H_2O_2 oxidation of rapidly-formed 408 nm peak in methanol at 25 °C. $[\mathbf{1}]_0 = 1.7$ to 4.1×10^{-6} mol dm^{-3}, $[H_2O_2]_0 = 4.2 \times 10^{-3}$ mol dm^{-3}.

where $(F_{20}TPP)Fe_{408}$ is the species formed at 408 nm. Eqn. (3) can be re-written as eqn. (4) in which k_d is the second-order rate

$$-dA/dt = \{(A'_0 - A_\infty)/[\mathbf{1}]_0\}k_d[H_2O_2][(F_{20}TPP)Fe_{408}] \quad (4)$$

constant for decomposition of $(F_{20}TPP)Fe_{408}$ and A'_0 is the decaying absorbance value interpolated back to $t = 0$.†† The value of $(A'_0 - A_\infty)/[\mathbf{1}]_0$ can be calculated as 120 000 ± 10 000. This gives a value for k_d of 0.073 ± 0.010 dm^3 mol^{-1} s^{-1} from the slope of Fig. 5 and of 0.068 ± 0.009 dm^3 mol^{-1} s^{-1} from Fig. 6. In addition, having found the reaction to be first order in each of catalyst and oxidant, the decomposition of the peak at 408 nm, after the initial period (see Fig. 4), can be analysed by a first-order method in the presence of a large excess of H_2O_2. Generally good first-order plots were obtained‡‡ (using the Guggenheim method in some cases)[13] and the observed rate constants are gathered in Table 3.

A plot of these k_{obs} values against $[H_2O_2]_0$ is linear (Fig. 7) giving a second-order rate constant k_d of 0.081 ± 0.004 dm^3 mol^{-1} s^{-1}, in good agreement with the value obtained from the initial-rate method.

Turning now to the rapid initial reaction; it is a reasonable assumption to treat this as the first of consecutive reactions in

†† Derivations of kinetic equations are shown in the supplementary material. See note †.

‡‡ See Figure Supp2 in the supplementary material. See note †.

Table 3 Values of observed first-order rate constant k_{obs} for decrease in absorbance at $\lambda = 408$ nm for the H_2O_2 oxidation of $(F_{20}TPP)FeCl$ (**1**) in methanol at 25 °C. $[\mathbf{1}]_0 = 4.1 \times 10^{-6}$ mol dm^{-3} [a]

Entry	$[H_2O_2]_0/10^{-3}$ mol dm^{-3}	$k_{obs}/10^{-4}$ s^{-1}
1	2.3	1.7 ± 0.1
2	4.7	4.3 ± 0.5
3	9.3	8.3 ± 0.8
4	14.1	11.5 ± 1.4
5	18.5	15.0 ± 0.2

[a] Omitting the small initial *increase* in absorbance due to formation of the 408 nm peak.

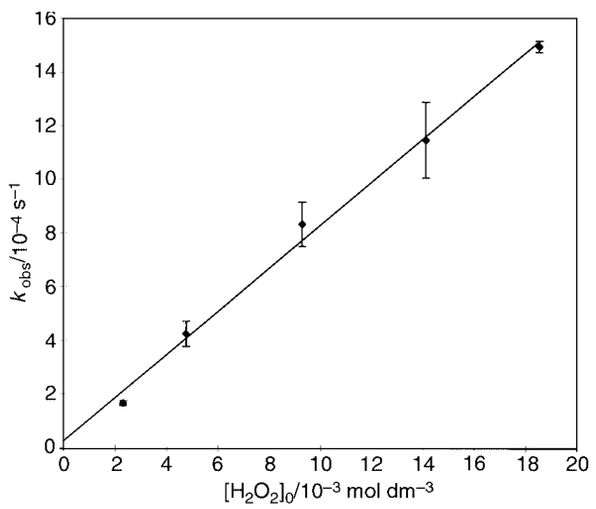

Fig. 7 Plot of k_{obs} *vs.* $[H_2O_2]_0$ for the H_2O_2 oxidation of rapidly-formed 408 nm peak in methanol at 25 °C. $[\mathbf{1}]_0 = 4.1 \times 10^{-6}$ mol dm^{-3}, $[H_2O_2]_0 = 2.3$ to 18.5×10^{-3} mol dm^{-3}.

which **1** (absorbing at 404 nm) is converted to $(F_{20}TPP)Fe_{408}$ (absorbing at *ca.* 408 nm) prior to the latter's decomposition (k_d) (Scheme 3).

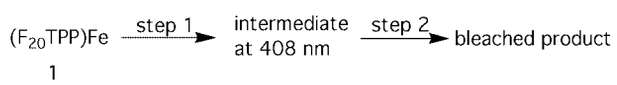

Scheme 3

Being too fast to analyse by the inital-rates method, it is necessary to assume a first-order dependance of the rate on **[1]** to obtain values for the first-order constant k^f_{obs}.§§ A cursory inspection of the *A vs.* time plots (*e.g.* Fig. 4) shows that the half-life for the first reaction is significantly shorter than that for the second. Under these conditions it can be shown that a plot of $\ln(A - A')$ *vs.* time, where A is the total absorbance at 408 nm at any time during the initial formation of the 408 nm peak and A' is the absorbance due to the second reaction (k_d) interpolated back into the region of the first (see inset to Fig. 4), yields as slope the first-order rate constant (k^f_{obs}) for the first reaction.¶¶ ||||

Repetition at different H_2O_2 concentrations yielded the range of values in Table 4 and a plot of these first-order rate constants k^f_{obs} *vs.* $[H_2O_2]_0$ shows a linear dependance and a *second-order* rate constant k_f calculated at 9.9 ± 1.1 dm^3 mol^{-1} s^{-1} (See Fig. 8).

§§ The observed first-order rate constant for the *formation* of $(F_{20}TPP)Fe_{408}$ is here called k^f_{obs} to distinguish it from the earlier k_{obs} for *decomposition* of $(F_{20}TPP)Fe_{408}$.

¶¶ Derivations of kinetic equations are shown in the supplementary material. See note †.

|||| See Figure Supp3 in the supplementary material. See note †.

Table 4 Values of observed first-order rate constant k^f_{obs} for initial rise of absorbance at $\lambda = 408$ nm for the H_2O_2 oxidation of $(F_{20}TPP)FeCl$ (**1**) in methanol at 25 °C. $[\mathbf{1}]_0 = 4.1 \times 10^{-6}$ mol dm^{-3}

Entry	$[H_2O_2]_0/10^{-3}$ mol dm^{-3}	k^f_{obs}/s^{-1}
1	0	0
2	2.1	0.022 ± 0.006
3	2.3	0.028 ± 0.012
4	4.2	0.043 ± 0.015
5	4.7	0.035 ± 0.003
6	8.2	0.086 ± 0.020

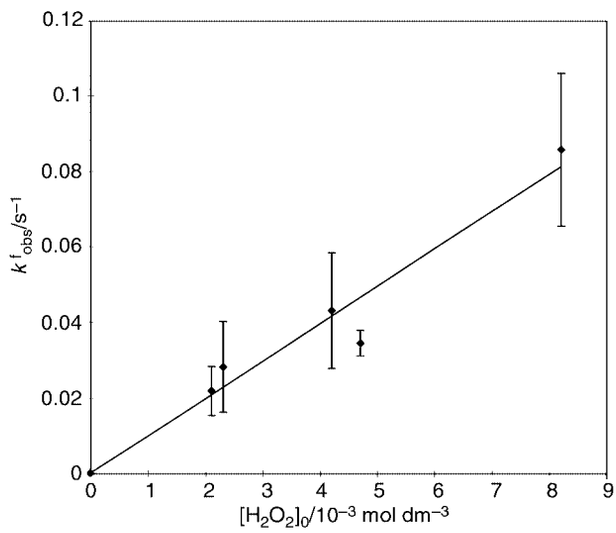

Fig. 8 Plot of k^f_{obs} *vs.* $[H_2O_2]_0$ for the formation of the 408 nm peak in the H_2O_2 oxidation of $(F_{20}TPP)FeCl$ (**1**) in methanol at 25 °C. $[\mathbf{1}]_0 = 4.1 \times 10^{-6}$ mol dm^{-3}, $[H_2O_2]_0 = 0$ to 8.2×10^{-3} mol dm^{-3}.

Discussion

The general mechanism shown in Scheme 2 for metalloporphyrin-catalysed alkene epoxidation is widely accepted. However, the nature of the 'oxidised intermediate' has been the subject of much debate especially when formed from reaction with hydrogen peroxide (as here) or hydroperoxides (ROOH). One school of thought favours an oxoferryl species (por)-Fe^{IV}=O [or its protonated form (por)Fe^{IV}–OH] formed by homolysis of the peroxide,[14] the other an oxoperferryl species (por)Fe^{V}=O,[2] or more likely, (por$^{\bullet+}$)Fe^{IV}=O formed by heterolysis (Scheme 4).

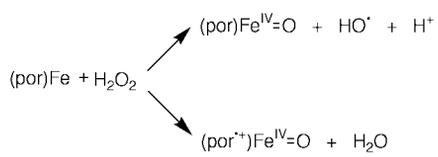

Scheme 4

Traylor has studied epoxidation by catalyst **1** with hydroperoxides and hydrogen peroxide and has presented convincing evidence for the *heterolysis* mechanism.[2,3a] In particular, the high yield and efficiency of the epoxidation reaction, as seen here for the hydroxynaphthoquinones **2,** is admitted even by those of the 'homolysis' school to be compelling evidence for the involvement (although not necessarily formed in the first or rate-limiting step) of the heterolysis intermediate (por$^{\bullet+}$)Fe^{IV}=O.[1a,15] A similar conclusion in favour of the intermediacy of (por$^{\bullet+}$)Fe^{IV}=O has been reached by Artaud and Mansuy for oxidation involving $(F_{20}TPP)FeCl$ and H_2O_2 under similar conditions to ours.[3b] The 'epoxidation factor', so

prominant here, is therefore difficult to reconcile with anything other than involvement of the (por$^{\bullet+}$)Fe^{IV}=O species in our oxidations of the hydroxynaphthoquinones. In light of this it is interesting to note that the value of the second-order rate constant k_1 obtained from the oxidation of the hydroxynaphthoquinone **2** at 22 ± 5 dm^3 mol^{-1} s^{-1} is significantly *lower* than the value of 190 ± 25 dm^3 mol^{-1} s^{-1} obtained by Traylor *et al.* from the oxidation of 2,4,6-tri-*tert*-butylphenol using the same catalyst, oxidant and solvent.[16] We have considered possible reasons for the discrepancy in values beginning with our kinetic Scheme 2 which is simpler than that of Traylor (Scheme 5).

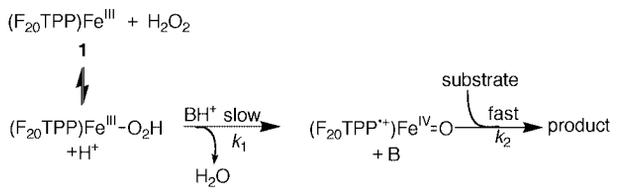

Scheme 5

This latter scheme proposes rate-limiting reaction of the initial complex (F_{20}TPP)Fe–O_2H under general acid catalysis by buffer (for certain hydroperoxides) or specific acid catalysis by lyonium ion (H_3O^+) in the presence of water (for H_2O_2) raising the possibility that substrate acidity may influence the rate-limiting-step. In our case the presence of *ca.* 10^{-4} mol dm^{-3} of the relatively strong (compared to water) acid **2**,[17] would be expected to *increase* the rate of the specific acid-catalysed k_1 step compared to that found by Traylor, who used the much weaker acid 2,4,6-tri-*tert*-butylphenol (albeit in much higher concentrations, up to 2000 × 10^{-4} mol dm^{-3}), and also the non-acidic β-carotene substrate. However, this might be cancelled by a decrease in the equilibrium concentration of (F_{20}TPP)Fe^{III}–O_2H with increased H_3O^+ concentration (see Scheme 5). On the other hand, the acid **2** would be expected to be a much better *general* acid than 2,4,6-tri-*tert*-butylphenol and might therefore speed up the k_1 step by general acid catalysis. In summary, we would expect substrate acidity, if relevant, to *increase* our oxidation rate constant relative to Traylor's (or at least to effect no change). In fact, our rate is *lower* and furthermore it shows little significant variation with substrate (**2**) (and therefore added acid) concentration.[18]

We believe, however, that an additional factor, oxidative destruction of the catalyst, a point often overlooked in such studies, is significant here. Even with a reactive substrate such as **2** which (by TLC analysis) leaves some unbleached catalyst at the reaction end, a degree of catalyst bleaching is found upon analysis of the reaction by UV-Vis spectroscopy. In a study of cyclooctene oxidation using catalyst **1** under conditions according to Traylor,[2] *ca.* 50% destruction of the catalyst was observed during the course of the reaction.[19] Clearly, such extensive destruction of catalyst makes kinetic analysis by a first-order approach less reliable, and we believe that our initial-rate method, where catalyst destruction is not (yet!) significant gives more reliable data. An alternative possibility is an inhibiting influence of substrate on the reaction of catalyst with oxidant, however, in this study we have seen no evidence for such an interaction.

In the absence of hydroxynaphthoquinone substrate the initial catalyst **1** (λ_{max} = 404, 485 and 580 nm, MeOH) is seen to be transformed into an intermediate **3** (λ_{max} = 408 and 550 nm, MeOH) before slower bleaching. The question arises as to the nature of the intermediate **3**, the transformations occurring during the bleaching process and its relevance to the substrate-oxidising catalytic cycle. Despite a wealth of literature reports on high-valent oxidised intermediates,[20] the identification of such species is still difficult. Much evidence points to the key species in the *epoxidation cycle* (*vide supra*) being the iron(IV) oxo radical cation porphyrin species, (F_{20}TPP$^{\bullet+}$)Fe^{IV}=O, but it is unlikely that our compound **3** is this species. Firstly, the UV-Vis spectrum is not typical of (por$^{\bullet+}$)Fe^{IV}=O; in particular there is no evidence for the absorption above 600 nm typical of the radical cation.[20] Furthermore, such oxoperferryl species are generally only seen at low temperature.[21] The UV-Vis spectrum of **3** suggests, particularly with the small peak *ca.* 550 nm, that **3** is the oxoferryl species (F_{20}TPP)Fe^{IV}=O.[22]

The kinetics of both formation and of destruction (bleaching) of **3** are interesting since both steps appear to be first-order in catalyst (or its derivative **3**) *and* H_2O_2. Intermediate **3** could be formed either *via* (F_{20}TPP$^{\bullet+}$)Fe^{IV}=O (Scheme 6, route *a* and *c*) *or* direct from **1** (Scheme 6 route *b*). The second-order rate

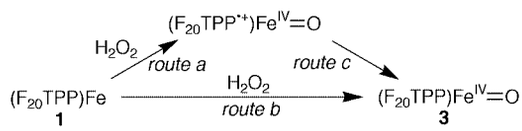

Scheme 6

constant k_f for formation of **3** in the *absence* of naphthoquinone **2** (9.9 ± 1.1 dm^3 mol^{-1} s^{-1}), although somewhat slower than the k_1 (22 ± 5 dm^3 mol^{-1} s^{-1}) obtained from the catalysed oxidation of hydroxynaphthoquinone **2** [which latter value we have argued reflects rate-limiting formation of the (F_{20}TPP$^{\bullet+}$)Fe^{IV}=O intermediate], *is* of the same order of magnitude. This is difficult to rationalise in terms of the simple Scheme 6 route *b* mechanism since the rate constant for this process would have to be much *faster* than that for route *a* in order to prefer route *b* formation of **3** [(F_{20}TPP)Fe^{IV}=O] over the route *a* formation of (F_{20}TPP$^{\bullet+}$)Fe^{IV}=O. Furthermore, the suggestion of Bruice that (por$^{\bullet+}$)Fe^{IV}=O is formed in a rapid step *subsequent to* rate-limiting formation of (por)Fe^{IV}=O is also ruled out by the observation of what appears to be almost quantitative buildup of **3** during the first minutes of the reaction, since under the Bruice mechanism **3** would be a 'steady-state' reactive intermediate.[15a]

The fact that the rate constant for formation of **3** is so close to that attributed to formation of (F_{20}TPP$^{\bullet+}$)Fe^{IV}=O, and that the rate depends on [H_2O_2], is best interpreted in terms of route *a* with rate-limiting oxidation of **1** to (F_{20}TPP$^{\bullet+}$)Fe^{IV}=O followed (route *c*) by rapid reduction to **3**. The most likely reductant is H_2O_2 itself; since this mechanism has been proposed by Traylor for other metalloporphyrins, *e.g.* (TMP)FeCl,*** to explain, among other things, the decrease in yield for perfluoroiodosylbenzene- or *m*-chloroperbenzoic acid-generated (por$^{\bullet+}$)Fe^{IV}=O alkene epoxidation in the presence of hydroperoxide *or* H_2O_2 (Scheme 7).[3b,23]

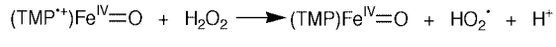

Scheme 7

This proposal is interesting since although Traylor quotes an estimated value of *ca.* 10^7 dm^3 mol^{-1} s^{-1} for the rate constant for reaction of (TMP$^{\bullet+}$)Fe^{IV}=O with H_2O_2, he found no significant H_2O_2 or RO_2H related reduction in epoxidation for catalyst **1**. Our findings suggests that, although undoubtedly slower than with (TMP$^{\bullet+}$)Fe^{IV}=O, (F_{20}TPP$^{\bullet+}$)Fe^{IV}=O *can* be reduced in this way with a rate constant of greater than 9.9–22 dm^3 mol^{-1} s^{-1}.

In the presence of excess H_2O_2 compound **3** is slowly bleached. In general the metalloporphyrin oxidative decomposition process is poorly understood. Quici *et al.* have noted

*** (TMP)FeCl = [5,10,15,20-tetrakis(2,4,6-trimethylphenyl)-21*H*,23*H*-porphine]iron(III) chloride.

three decomposition routes for oxidised metalloporphyrins such as **3**: (i) oxidative decomposition of the porphyrin ring, (ii) formation of μ-oxo dimers and (iii) 'suicide inhibition' *i.e.* reaction of the substrate (or an intermediate) with the porphyrin ring.[1b] In addition a mechanism involving nucleophilic attack on an oxidised metalloporphyrin intermediate has been proposed.[24] The use of metallo*tetra*arylporphyrins with *ortho* substituents to the aryl ring is a well-established tactic to reduce dimer formation,[25] while the use of electron-withdrawing substituents to the aryl ring is believed to reduce (unspecified) oxidative catalyst destruction.[25] Decompositions by oxidation of the porphyrin ring are the least well characterised, but an important mode appears to involve reaction of the *unoxidised* metalloporphyrin with an oxidised form such as (por)Fe^{IV}=O (*e.g.* **3**)[26] or (por$^{\bullet+}$)Fe^{IV}=O.[27] However, being bimolecular, this mode can be suppressed by the use of sterically-hindered (*e.g. ortho*-substituted *meso*-aryl groups) metalloporphyrins.[28] In the present work the lack of second-order dependance of the [catalyst] precludes this as a major decomposition route for **3**. Furthermore, an intramolecular 'self-oxidation', initiated for example by rearrangement of the oxoferryl **3** to an iron porphyrin *N*-oxide,[26b,29] would show a first-order dependence on **[3]** *only*. Instead, the kinetic dependance of the decomposition of **3** on the $[H_2O_2]$ indicates an oxidative decomposition of **3** which probably involves oxidation of the porphyrin ring by H_2O_2; this is *despite* the presence of the strongly electron-withdrawing pentafluorophenyl *meso*-substituents. This is a decomposition route which is not commonly cited, although it has been proposed for decomposition of haem undecapeptide (microperoxidase 11).[30] Indeed, for hydroperoxides, a *reductive* reaction with ferryl species (por)Fe^{IV}=O leading to regeneration of (por)Fe^{III} is more often proposed.[3b,31]

Conclusions

In conclusion we have shown that the rate-limiting step in the (F_{20}TPP)FeCl-catalysed H_2O_2 oxidation of hydroxynaphthoquinones is formation of an oxidised metalloporphyrin intermediate. The results also provide further support for this being an oxoperferryl species, ($F_{20}TPP^{\bullet+}$)Fe^{IV}=O, but formed with a rate constant for formation significantly slower than previously quoted. In the absence of hydroxynaphthoquinone substrate, the ferryl species, (F_{20}TPP)Fe^{IV}=O, is the predominant oxidised intermediate, most likely formed *via* ($F_{20}TPP^{\bullet+}$)Fe^{IV}=O. Finally, this intermediate decomposes *via* H_2O_2 oxidation, probably of the porphyrin ring, to give a bleached product.

References

1 (*a*) B. Meunier, *Chem. Rev.*, 1992, **92**, 1411; (*b*) S. Quici, S. Banfi and G. Pozzi, *Gazz. Chim. Ital.*, 1993, **123**, 597; (*c*) C. K. Chang and F. Ebina, *J. Chem. Soc., Chem. Commun.*, 1981, 778.
2 T. G. Traylor, C. Kim, J. L. Richards, F. Xu and C. L. Perrin, *J. Am. Chem. Soc.*, 1995, **117**, 3468.
3 (*a*) T. G. Traylor, S. Tsuchiya, Y.-S. Byun and C. Kim, *J. Am. Chem. Soc.*, 1993, **115**, 2775; (*b*) I. Artaud, K. Ben-Aziza and D. Mansuy, *J. Org. Chem.*, 1993, **58**, 3373; (*c*) G. J. Harden and M. M. Coombs, *J. Chem. Soc., Perkin Trans. 1*, 1995, 3037; (*d*) E. Baciocchi, O. Lanzalunga and A. Lapi, *Tetrahedron. Lett.*, 1995, **36**, 3547.
4 J. E. Lyons, P. E. Ellis Jr. and H. K. Myers Jr., *J. Catal.*, 1995, **155**, 59.
5 J. R. Wolf, C. G. Hamaker, J.-P. Djukic, T. Kodadek and K. L. Woo, *J. Am. Chem. Soc.*, 1995, **117**, 9194.
6 E. Baciocchi and M. Ioele, *J. Org. Chem.*, 1995, **34** 4896.
7 G. Harden, *J. Chem. Soc., Perkin Trans. 2*, 1995, 1883.
8 M. Takeuchi, M. Kodera, K. Kano and Z. Yoshida, *J. Mol. Catal. A: Chem.*, 1996, **113**, 51.
9 R. Iwanejko, P. Battioni, D. Mansuy and T. Mlodnicka, *J. Mol. Catal. A: Chem.*, 1996, **111**, 7.
10 K. A. Lee and W. Nam, *J. Am. Chem. Soc.*, 1997, **119**, 1916; A. K. Le and W. Nam, *Bull. Korean Chem. Soc.*, 1996, **17** 669.
11 B. Pietzyk, L. Froehlich and B. Goeber, *Pharmazie*, 1996, **51**, 654; B. Pietzyk, L. Froehlich and B. Goeber, *Pharmazie*, 1995, **50**, 747.
12 I. D. Cunningham, T. N. Danks, K. T. A. O'Connell and P. W. Scott, *J. Org. Chem.*, in press. Compound **2** is oxidised across the C2,C3 C=C to yield an epoxide, identified in crude form from its NMR spectrum. This epoxide further reacts with unreacted **2** and methanol to yield 2° products which have been characterised and which can only arise from an epoxide. The only 2° product likely to show UV-Vis absorbance similar to **2** is a 'dehydro-dimer', but this only forms in much more concentrated solutions of **2** than used here.
13 B. G. Cox, *Modern Liquid Phase Kinetics*, Oxford University Press, Oxford, 1994.
14 T. C. Bruice, *Acc. Chem. Res.*, 1991, **24**, 243; E. Gopinath and T. C. Bruice, *J. Am. Chem. Soc.*, 1991, **113**, 4657, 6090, 6095; R. Panicucci and T. C. Bruice, *J. Am. Chem. Soc.*, 1990, **112**, 6063; P. Battioni, J. P. Renaud, J. F. Bartoli, M. Reina-Artiles, M. Fort and D. Mansuy, *J. Am. Chem. Soc.*, 1988, **110**, 8462; D. Mansuy, *Pure Appl. Chem.*, 1987, **59**, 759.
15 (*a*) K. Murata, R. Panicucci, E. Gopinath and T. C. Bruice, *J. Am. Chem. Soc.*, 1990, **112**, 6072; (*b*) G.-X. He and T. C. Bruice, *J. Am. Chem. Soc.*, 1991, **113**, 2747.
16 See ref. 2. A similar value was obtained using the alkene β-carotene.
17 pK_a values (in H_2O) for hydroxynaphthoquinones are typically 4–5, see L. Fieser and M. Fieser, *J. Am. Chem. Soc.*, 1934, **56**, 1565.
18 Indeed, Traylors own results [see refs. 2 and 3(*a*)], which show the *same* rate constant for use of 2,4,6-tri-*tert*-butylphenol or β-carotene (the former at levels probably high enough to add significantly to levels of H_3O^+) appear to rule out a lyonium ion effect.
19 I. D. Cunningham, B. G. Cox, J. N. Hay, I. Hamerton, T. N. Danks and S. Gunathilagan, unpublished work.
20 A definitive description of the UV-Vis changes associated with the formation of high-valent iron oxo porphyrin complexes is hard to find, particularly with respect to the Soret band. The situation is complicated by solvent variations and variations due to ligation by solvent and added ligands. Furthermore ligation can be differential for the various oxidised states. (*a*) J. T. Groves and Y. Watanabe, *J. Am. Chem. Soc.*, 1986, **108**, 7834; (*b*) J. T. Groves, R. C. Haushalter, M. Nakamura, T. E. Nemo and B. J. Evans, *J. Am. Chem. Soc.*, 1981, **103**, 2884; (*c*) J. T. Groves and Y. Watanabe, *J. Am. Chem. Soc.*, 1986, **108**, 507; (*d*) S. Hashimoto, Y. Tatsuno and T. Kitagawa, *J. Am. Chem. Soc.*, 1987, **109**, 8096; (*e*) A. Gold, K. Jayaraj, P. Doppelt, R. Weiss, G. Chottard, E. Bill, X. Ding and A. X. Trautwein, *J. Am. Chem. Soc.*, 1988, **110**, 5756; (*f*) H. Sagimoto, H.-C. Tung and D. T. Sawyer, *J. Am. Chem. Soc.*, 1988, **110**, 2465; (*g*) K. Yamaguchi, Y. Watanabe and I. Morishima, *J. Chem. Soc., Chem. Commun.* 1992, 1721; (*h*) N. Colclough and J. R. Lindsay Smith (see among others *J. Chem. Soc., Perkin Trans. 2*, 1994, 1139). In summary, it appears that (i) conversion to the (por$^{\bullet+}$)Fe^{IV}=O usually gives a Soret band *ca.* 406 nm, *but with* $\varepsilon \approx 50\%$ *of the original and a small peak ca. 680 nm* and (ii) conversion to (por)Fe^{IV}=O seems to give a Soret band at 406–426 nm, but also a small band *ca.* 550 nm.
21 H. Fuji, *Chem. Lett.*, 1994, 1491.
22 Typical UV-Vis spectra for oxoferryl porphyrins are shown in ref. 20(*h*) and references therein.
23 T. G. Traylor and F. Xu, *J. Am. Chem. Soc.*, 1987, **109**, 6201.
24 K. R. Bretscher and P. Jones, *J. Chem. Soc., Dalton Trans.*, 1988, 2273.
25 P. S. Traylor, D. Dolphin and T. G. Traylor, *J. Chem. Soc., Chem. Commun.*, 1984, 279.
26 (*a*) M. J. Nappa and C. A. Tolman, *Inorg. Chem.*, 1985, **24**, 4711; (*b*) D. R. Leonord and J. R. Lindsay Smith, *J. Chem. Soc., Perkin Trans. 2*, 1991, 25.
27 K. R. Bretscher and P. Jones, *J. Chem. Soc., Dalton Trans.*, 1988, 2267.
28 S. E. J. Bell, P. R. Cooke, P. Inchley, D. R. Leonord, J. R. Lindsay Smith and A. Robbins, *J. Chem. Soc., Perkin Trans. 2*, 1991, 549.
29 J. T. Groves and Y. Watanabe, *J. Am. Chem. Soc.*, 1986, **108**, 7836.
30 G. M. Clore, M. R. Hollaway, C. Orengo, J. Peterson and M. T. Wilson, *Inorg. Chim. Acta*, 1981, **56**, 143.
31 J. R. Lindsay Smith and R. J. Lower, *J. Chem. Soc., Perkin Trans. 2*, 1991, 31.

Paper 9/03511G